

ORIGINAL STUDIES

Differences in rotational positioning and subsequent distal main branch rewiring of the Tryton stent: An optical coherence tomography and computational study

Maik J. Grundeken, MD, PhD¹  | Claudio Chiastra, PhD²  | Wei Wu, PhD^{2,3} |

Joanna J. Wykrzykowska, MD, PhD¹ | Robbert J. De Winter, MD, PhD¹ |

Gabriele Dubini, PhD² | Francesco Migliavacca, PhD²

¹Department of Cardiology, Academic Medical Center, University of Amsterdam, Amsterdam, The Netherlands

²Laboratory of Biological Structure Mechanics, Department of Chemistry, Materials and Chemical Engineering "Giulio Natta," Politecnico di Milano, Milan, Italy

³Department of Mechanical Engineering, University of Texas at San Antonio, San Antonio, TX

Correspondence

Claudio Chiastra, PhD, Laboratory of Biological Structure Mechanics, Department of Chemistry, Materials and Chemical Engineering "Giulio Natta," Politecnico di Milano, Piazza Leonardo da Vinci 32, 20133 Milan, Italy.
Email: claudio.chiastra@polimi.it

ABSTRACT

Objectives: To evaluate the occurrence of rewiring through one of the panels of the Tryton stent (instead of the assumed re-wiring in-between the panels) and the influence on stent geometry and mechanics.

Background: Tryton is a side branch stent used in combination with a main branch device. It is placed without the need of rotational orientation. However, it is unknown whether main branch re-wiring accidentally may occur through a panel, instead of in-between the panels.

Methods: We used three-dimensional optical coherence tomography to evaluate the location of distal main branch re-wiring through Tryton. Furthermore, we used computer simulations to evaluate the influence on stent geometry and mechanics.

Results: Rewiring through a panel (instead of in-between two panels) occurred in 45% of the cases. By using virtual stent deployment, we found minimal differences in ostial side branch stenoses (44.8% in-between the panels and 39.0% through a panel). There were no differences in minimum stent areas of the distal main branch (6.38 mm² vs. 6.39 mm²). In both scenarios, the re-wired Tryton cell was large enough for main branch stenting (expressed as the diameter of the largest possible circle that fits within the cells): 3.40 mm (in-between the panels) vs. 3.02 mm (through a panel).

Conclusions: In 45% of the Tryton implantations, distal main branch rewiring (and subsequent main branch stenting) was performed through one Tryton panel, instead of the assumed rewiring in-between the panels. However, this did not result in unfavorable stent geometries or mechanics, as evaluated with computer simulations.

KEYWORDS

computer simulation, coronary bifurcation, dedicated stent, intravascular imaging, optical coherence tomography, virtual bench testing

Abbreviations: 3D, three-dimensional; D1, first diagonal branch; FDA, Food and Drug Administration; IFU, instructions for use; LAD, left anterior descending coronary artery; OCT, optical coherence tomography; PCI, percutaneous coronary intervention; POT, proximal optimization technique; QCA, quantitative coronary angiography; RCA, right coronary artery; RCx, ramus circumflex.

Maik J. Grundeken and Claudio Chiastra contributed equally to this work.

1 | INTRODUCTION

The Tryton Side Branch StentTM has been developed for a "simplified culotte" technique with the hope to improve outcomes of percutaneous coronary interventions (PCIs) of bifurcation lesions [1,2]. The Tryton stent shares its proximal part with the main branch stent proximal

to the bifurcation. The Tryton stent consists of three zones [1,2]: a proximal main branch zone, the central transition zone, and a distal side branch zone. The proximal main branch zone has two proximal “wedding bands”, from which three undulating fronds connect these wedding bands with three “panels” of the transition zone. This part of the stent has a minimal amount of metal, resulting in large sized cells, enclosed by the distal margin of the wedding bands, the undulating fronds, and the proximal margins of the panels. The potential benefit of this design is that due to these large sized cells, main branch re-wiring and main branch stent implantation (after Tryton implantation, which is performed first) will become easier and the so called ‘napkin ring’ effect may be avoided [3,4].

The Tryton stent is placed without (the need of) rotational orientation. However, it is unknown whether main branch rewiring accidentally may occur through one of the panels, instead of through the large sized cells. Moreover, if this may occur, it is unknown what the impact will be on the mechanical behavior of the Tryton stent. Therefore, we performed a study using three-dimensional (3D) reconstructions of optical coherence tomography (OCT) pullbacks to evaluate the occurrence in vivo of main branch rewiring through the panels (instead of through the large cells in-between the undulating fronds, distal wedding band and proximal margins of the panels). Furthermore, we performed virtual stent deployment in a bifurcation model to investigate the influence of main branch stent placement through the panels on Tryton stent mechanics.

2 | METHODS

2.1 | Device

The Tryton Side Branch StentTM is discussed in detail elsewhere [1,2]. Briefly, it is a cobalt-chromium bare metal stent with a strut thickness of 84 μm (0.0033 in.). It is a slotted-tube, balloon-expandable stent and is 5 or 6 Fr compatible (depending on the size used), delivered using a single rapid exchange system over a conventional 0.014-in. guidewire. The stent is mounted on a single delivery balloon which is tapered with a larger proximal than distal diameter [1,2].

The Tryton stent consists of three zones. The distal side branch zone has a conventional tubular stent design with out-of-phase zigzag hoops connected with one link per crown. The second zone is the transition zone with three panels that can be independently deformed to adjust to a wide range of bifurcation anatomies. The third zone is the proximal main branch zone which has two “wedding bands” to mount the proximal part of the stent on the delivery balloon and to “anchor” the stent in the proximal main branch after implantation. The wedding bands are connected with the panels of the transition zone by three undulating struts. Because of this design there is a minimal amount of metal in the proximal main branch, with a large cell size in-between the most distal wedding band, the undulating struts, and the proximal margin of the panels. This theoretically allows easy delivery of a conventional stent, through the Tryton stent, in the main branch, avoiding problems with deployment of the main branch stent (such as the “napkin ring” effect).

The stent deployment sequence, as recommended by the manufacturer, is described in the instructions for use (IFU). First, both branches (main and side branch) are wired. Predilatations of the main branch and/or side branch are performed at the discretion of the operator. Hereafter, the Tryton stent is advanced into the side branch and positioned using the four radio-opaque markers on the stent delivery system [1,2]. The stent is positioned in such a way that the carina lies in-between the two middle markers, without the need for rotational orientation. After stent deployment, it is recommended to perform a proximal optimization technique (POT) by dilatation of the proximal main branch zone to ensure adequate apposition of the wedding bands to the vessel wall. Then, the side branch wire, used for Tryton stent delivery, is retracted and advanced through the Tryton stent into the distal main branch. To avoid rewiring in-between the Tryton stent cells and the vessel wall, the side branch wire is not further retracted than the proximal main branch zone (proper rewiring may be further facilitated by leaving the tip of the balloon catheter used for the POT in the proximal main branch; also known as the “Stella Manoeuvre”). Rewiring is facilitated by the large sized cells in-between the distal margin of the distal wedding band, the undulating fronds, and the proximal margins of the panels in the transition zone. The “trapped” main branch wire could then be retracted. Subsequently, a balloon is advanced over the rewired main branch wire, through the Tryton stent, to predilate the main branch. After dilatation, a conventional tubular stent is advanced, crossing the side branch, and deployed in the main branch. Finally, the side branch is rewired through the main branch stent and a final kissing balloon dilatation is performed. Ideally, the procedure is finished with a final POT to correct for the oval-shaped stent distortions in the proximal main branch created by overlap of the kissing balloons in the proximal main branch [5].

The stent is commercially available in multiple countries within Europe (CE marked since 2008), Middle East and Africa, and recently the Food and Drug Administration (FDA) granted approval for its use in the United States.

2.2 | Three-dimensional optical coherence tomography

We used OCT data from two observational studies to evaluate where the Tryton stent was rewired (through a large sized cell in-between the panels or through a panel). The first study was a follow-up study using quantitative coronary angiography (QCA) and OCT to evaluate the performance of the Tryton stent [6]. All patients provided written informed consent prior to the repeat angiography. In the second study we reported clinical, QCA, and OCT data on 10 patients which were treated for bifurcation lesions with the Tryton stent in combination with the Absorb bioresorbable vascular scaffold (BVS) (Abbott Laboratories, Abbott Park, IL) [7]. The necessity to obtain written informed consent was waived by the institutional review committee because the procedures were performed as part of routine clinical care (both devices were CE-marked).

OCT pullbacks were performed with the Illumien frequency-domain system (St Jude Medical, St Paul, MN). After advancing the

OCT imaging catheter over a conventional, 0.014-in. guidewire, pullbacks were performed during continuous X-ray contrast injection of 4 mL sec⁻¹ at a maximum pressure of 300 psi using an injection pump. Images were acquired at 100 frames s⁻¹ at a pullback speed of 20 mm s⁻¹. Calibration was performed based on the reflection of the imaging catheter. From every OCT pullback, each individual strut was detected by hand in each OCT frame. Hereafter, 3D-OCT images were reconstructed offline using the volume rendering software AMIRA (FEI, Hillsboro, OR) [7,8]. For every 3D-OCT reconstruction, the site of distal main branch fenestration was scored visually by one of the investigators (MJG) as follows:

1. "in-between two panels," through the large sized cells which are enclosed by the distal wedding band, the undulating fronds and the proximal margin of the panels; and
2. "through the panel," in which the distal main branch rewiring was performed through a cell of one of the panels.

2.3 | Virtual stent deployment

A bifurcation model of the left anterior descending (LAD) coronary artery with its first diagonal (D1) branch was used for the virtual Tryton stent placement. The geometry of the bifurcation model was based on the clinical literature [9]. The lumen diameters of the three branches obeyed Finet's law [10] and were 3.50 mm (proximal main branch), 2.76 mm (distal main branch), and 2.40 mm (side branch), respectively. The distal bifurcation angle was set to 45° while the proximal-to-distal main branch angle was set to 180°. The vessel wall thickness was defined as the 30% of the lumen diameters according to experimental measurements [11]. The vessel wall was divided into three layers, namely intima, media, and adventitia. The material of each layer was modeled using an isotropic hyperelastic constitutive law based on *ex vivo* experimental data on human coronary specimens [11], in accordance with previous studies [12,13].

A validated model of the Tryton stent (length of 19 mm and step delivery system of 2.5–3.5 mm) was used. Details of this model are reported elsewhere [14]. Briefly, the cobalt-chromium alloy that characterizes the stent was defined as an elasto-plastic isotropic material. The polymeric material of the balloon was described by means of an elastic linear isotropic model. Two different elastic moduli were assigned to the proximal and distal parts of the balloon to comply with the manufacturer pressure-diameter relationship. The model of the Tryon stent was validated by comparing an experimental free-expansion with the corresponding computer simulation.

Models of the 3 × 15 mm Xience V stent (Abbott Laboratories) [13] and NC Sprinter RX noncompliant balloon (Medtronic, Fridley, MN) (sizes 2.5 × 15 mm, 3 × 15 mm, and 3.5 × 9 mm) were also created. All balloon models were calibrated to replicate the manufacturer pressure-diameter curve following the same procedure used for the Tryton step balloon [14].

Two different experiments were performed with virtual stent placements of the Tryton stent in combination with the Xience V stent.

The two scenarios were simulated in the bifurcation model using the finite element software ABAQUS/Explicit (Dassault Systèmes Simulia Corp., Providence, RI). Simulation settings were those adopted in previous studies from our group [12,13,15]. In the first virtual stent placement experiment, we assumed an ideal scenario (with rewiring "in-between two panels") and the deployment sequence consisted of the following steps, in agreement with the IFU (Figure 1):

1. Insertion of a 19 × 2.5, 3.5 mm Tryton stent in the side branch;
2. Expansion of the Tryton stent at 10 atm;
3. POT by expanding a 3.5 × 9 mm balloon at 8 atm;
4. Rewiring from the proximal to distal main branch in-between two panels of the Tryton stent, through one of the large sized cells;
5. Insertion of a 3 × 15 mm NC Sprinter RX balloon from the proximal to distal main, through the Tryton stent struts;
6. Inflation of this balloon at 8 atm to allow main branch stent delivery;
7. Insertion of a 3 × 15 mm Xience V in the main branch, through the Tryton stent;
8. Deployment of the Xience V stent (9 atm);
9. Final kissing balloon dilatation by expanding 2.5 × 15 mm and 3 × 15 mm NC Sprinter RX balloon balloons at 8 atm in the side branch and main branch, respectively;
10. Finalization of the procedure with a POT by expanding a 3.5 × 9 mm NC Sprinter RX balloon at 9 atm.

In the second virtual stent placement experiment, we assumed that after Tryton stent placement, one of the panels was located in front of the distal main branch ostium. The deployment sequence and the subsequent steps were identical as described above with the exception that main branch rewiring (step 4) was performed through one of the panels instead of through the large sized cells in-between two panels (Figure 2).

The two scenarios were compared by quantifying geometrical changes after stenting procedure. The side branch ostial area stenosis (expressed as percentage) was calculated as follows [16]: (total side branch ostium surface area – largest area free from struts)/total side branch ostium surface area × 100. The minimum stent area at the distal main branch ostium was defined as the cross-sectional inner lumen stent area without considering the stent struts [17]. The minimum lumen diameter at the distal main branch ostium was calculated as the cross-sectional minimum diameter from one strut edge to the opposite one [17]. The malapposition area was defined as the percentage of stent area with malapposed stent struts with respect to the total stent area. The geometries of the deployed Tryton stents were compared by evaluating the cell opening of the large sized cells of the proximal zone and the panels of the transition zone of the device. The diameter of the largest possible circle which fits within the stent cell struts was used as an estimate of the cell opening [17].

In addition to geometrical changes after stenting, the arterial wall stress (expressed as maximum principal stress) and the stress in the stents (expressed as von Mises stress) were calculated as previously reported [18].

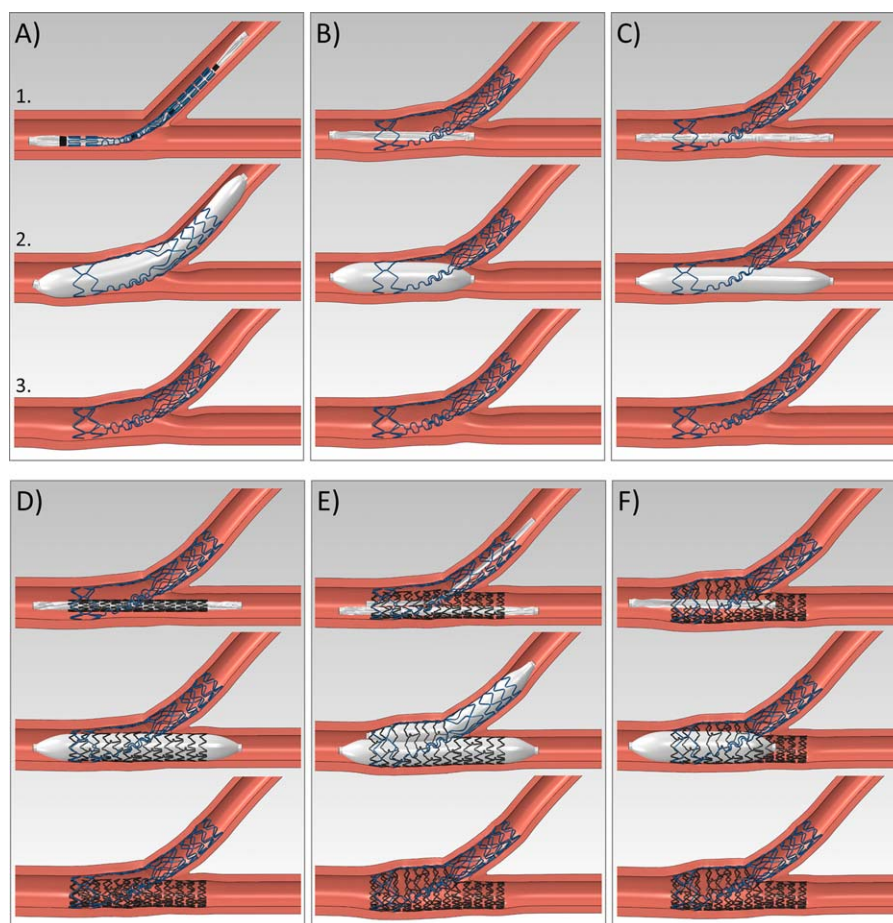


FIGURE 1 Virtual deployment sequence of the Tryton stent in combination with the Xience V stent in a left anterior descending/first diagonal coronary bifurcation model. A, Expansion of the Tryton stent in the side branch. B, Proximal optimization technique. C, Opening of the main branch access. D, Expansion of the Xience V stent in the main branch. E, Kissing balloon inflation. F, Proximal optimization technique. For each step, (1) insertion, (2) expansion, and (3) recoil of the balloon/stent is shown [Color figure can be viewed at wileyonlinelibrary.com]

3 | RESULTS

3.1 | Three-dimensional optical coherence tomography

From the 20 patients available, 11 were suitable for the current analysis (Figure 3). In nine cases it was not possible to assess the location of distal main branch rewiring. All these cases were from the Tryton OCT follow-up study in which the Tryton stent was used in combination with a metallic stent in the main branch. Therefore, the Tryton stent could not be distinguished from the metallic main branch stent, which prevented 3D-OCT reconstruction of the Tryton stent. One case from this study was suitable for the current analysis since in this case Tryton was used to treat a Medina 0,0,1 lesion without the placement of a main branch stent [19]. Therefore, we were able to 3D reconstruct the Tryton stent during the follow-up OCT, even though it was covered with some neointima. We were able to use all cases (all OCTs were from baseline pullbacks) from the Tryton-Absorb registry, because the metallic Tryton struts could be distinguished from the polymeric Absorb struts.

From these 11 patients, in only 5 (45%) patients main branch re-wiring was performed through the large sized cells, in-between the panels (a case example is shown in Figure 4 and Supporting Information video 1). In 5 (45%) other cases, main branch re-wiring was performed through one of the panels (a case example is shown in Figure 5 and Supporting Information video 2). In the remaining case (9%), main branch rewiring occurred even further, distal to the panels of the middle zone.

3.2 | Virtual stent deployment

Figure 6A shows a cross-sectional view of the side branch ostium for the two investigated scenarios. The side branch ostial area stenosis was numerically larger in the case with correct main branch rewiring (in-between two panels) than in that with main branch re-wiring “through a panel” (44.8% versus 39.0%, respectively). The minimum stent area at the distal main branch ostium was similar in both scenarios (6.38 and 6.39 mm² for the cases with correct re-wiring and main branch re-wiring through a panel, respectively) (Figure 6B). Similarly, comparable values of minimum lumen diameter were found at the

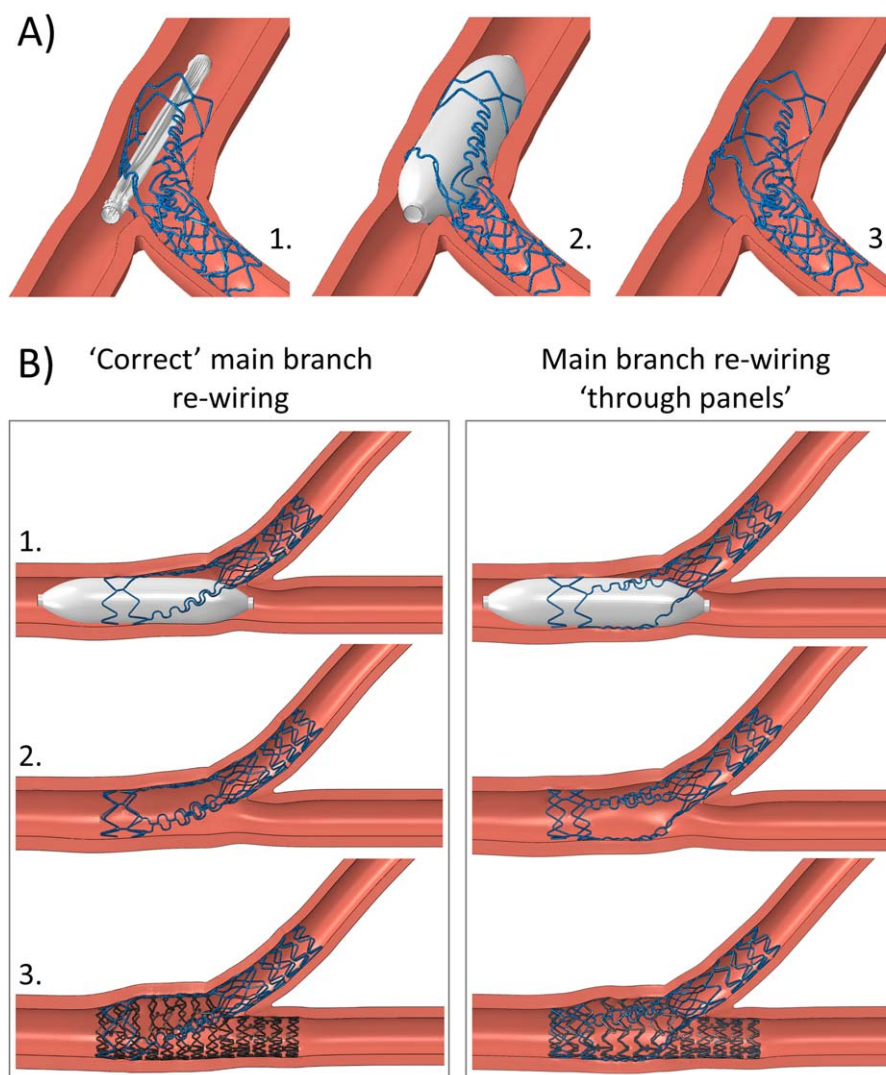


FIGURE 2 Main branch rewiring after Tryton stent implantation. A, Rewiring through one of the panels of the stent: (1) insertion of the balloon, (2) expansion, and (3) recoil after balloon deflation. B, Comparison between the “correct” rewiring and the rewiring “through panels”: (1) expansion of the balloon, (2) recoil after balloon deflation, and (3) geometrical configuration at the end of the procedure [Color figure can be viewed at wileyonlinelibrary.com]

distal main branch ostium for the two analyzed cases (2.82 mm for both cases).

Malapposed struts are indicated in red in Figure 6C for both scenarios. The malapposition area was numerically smaller in the case with rewiring in-between two panels (18.7% versus 20.3%, respectively). The percentage of malapposed area at the side branch ostium with respect to the total malapposed area was 19.2% in the case with rewiring in-between two panels and 14.9% in that with re-wiring through a panel.

In Figure 7 the Tryton stent geometry at the end of the procedure is compared for the two investigated scenarios. The cell opening of the large sized cells of the proximal zone and the panels of the transition zone of the device is reported in Table 1. The assumed main branch rewiring in-between panels induces a uniform expansion of the stent cells in the proximal and transition zones of the device, with a well-opened large cell in-between the panels (through which the main branch stent

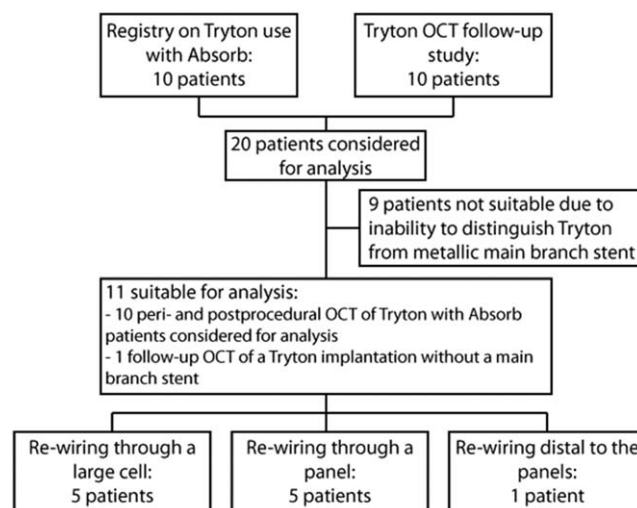


FIGURE 3 Flowchart reporting the patients included in the analysis

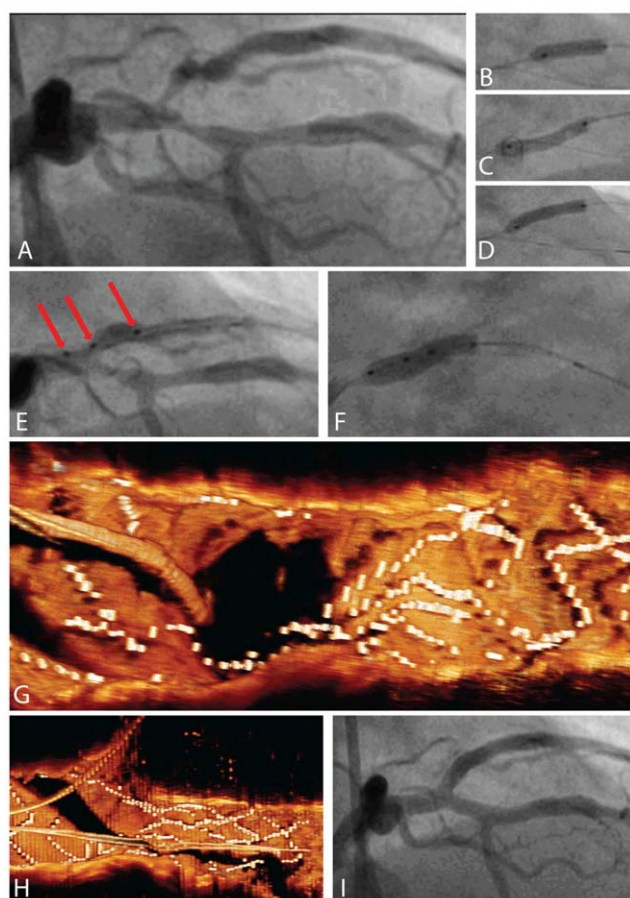


FIGURE 4 Clinical example of “correct” main branch rewiring. This case example was a 53-year-old male with recent STEMI for which he underwent a primary PCI with drug-eluting stent placement in the ramus circumflex (RCx). A, angiography showed a distal LAD lesion and a Medina 1,1,1 lesion of the LAD/D1 bifurcation. The distal LAD was treated with a bioresorbable vascular scaffold (not shown). B,C, then, the D1 was predilated. D, hereafter, an Absorb BVS was implanted in the D1. E, a $3.5\text{--}3.0 \times 15\text{ mm}^2$ Tryton was positioned from the proximal LAD into the D1 using the four radiopaque markers on the delivery system (red arrows; most proximal marker not visible). F, Tryton was deployed at 10 atm, overlapping with the previously placed BVS. G, 3D-OCT reconstruction from a pullback from the side branch to the proximal main branch shows precisely how re-wiring of the guidewire into the distal main branch is in-between the undulating fronds (“correct” rewiring). H, 3D-OCT reconstruction from the same pullback as in “G,” but from a view perpendicular at the distal main branch ostium. I, final angiographic result after main branch BVS implantation [Color figure can be viewed at wileyonlinelibrary.com]

is implanted) with a diameter of the largest possible circle of 3.40 mm (Figure 7, Circumference A). Main branch re-wiring through a panel induces a high distortion of one of the panels of the transition zone of the Tryton stent, resulting in a stent cell diameter of 3.02 mm (Figure 7, Circumference D), which is approximately three times larger than the other cells of the other panels (Figure 7, Circumferences E,F). The stent cell diameter of 3.02 mm however is well beyond the 2.76 mm of the distal main branch diameter.

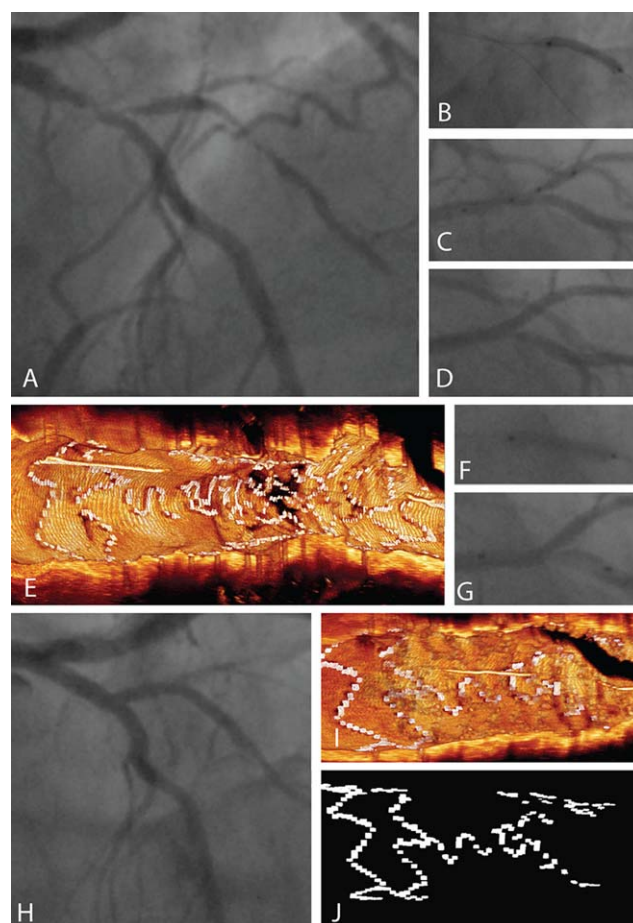


FIGURE 5 Clinical example of main branch rewiring “through a panel.” This case example was a 48-year-old male with a history of PCI of the right coronary artery (RCA) and ramus circumflex (RCx) branch. He presented with progression of his stable angina with an exercise test suggestive for ischemia in the anterolateral wall. Diagnostic angiography showed a chronic total occlusion of the RCA, patent stents in the RCx (not shown) and, as displayed in panel A, a bifurcation lesion of the LAD-D1 branch with a second subtotal stenosis in D1. A PCI was performed. First, both branches were wired. B, then, the side branch was treated, after predilatation, with a $2.5 \times 18\text{ mm}^2$ Absorb BVS. C, hereafter, a $3.5\text{--}2.5 \times 19\text{ mm}^2$ Tryton stent was positioned using the four radiopaque markers on the delivery system. Panel D shows the angiogram after deployment of the Tryton stent. An OCT pullback from the side branch to the proximal main branch was performed. E, 3D reconstruction of this pullback shows that one of the three panels of the Tryton stent is located just before the ostium of the distal main branch. F, the main branch was re-wired and a main branch balloon dilatation was performed with a $3.0 \times 15\text{ mm}$ NC Trek balloon. G, This is followed by implantation of a $3.0 \times 18\text{ mm}^2$ Absorb BVS (10 atm). Final kissing balloon dilatation was not performed in this case. H, the final angiogram shows a good angiographic result. I, 3D reconstruction of a final OCT pullback from distal-to-proximal main branch showing how the struts of the panels are widened after main branch dilatation and BVS placement through the panel (BVS struts not colored). J, 3D reconstruction of the Tryton stent from the same viewing angle as in panel “I,” now without BVS and without vessel wall behind. Note that the distal side branch part of the Tryton stent could not be visualized in panels “I” and “J” because these 3D reconstructions are obtained from a main branch pullback [Color figure can be viewed at wileyonlinelibrary.com]

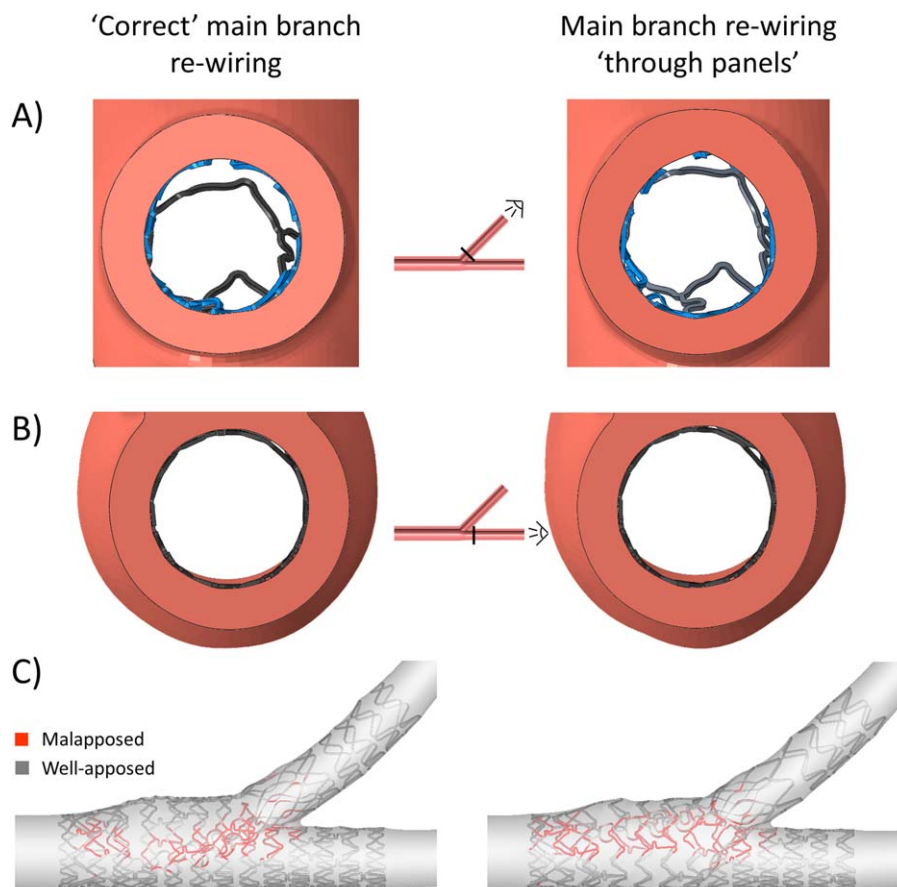


FIGURE 6 Comparison of the two investigated scenarios in terms of geometrical changes at the end of the stenting procedure. A, Cross-sectional view of the side branch ostium from the side branch extremity. B, Cross-sectional view of the distal main branch ostium from the distal main branch extremity. C, Quantification of stent strut malapposition; malapposed struts are highlighted in red [Color figure can be viewed at wileyonlinelibrary.com]

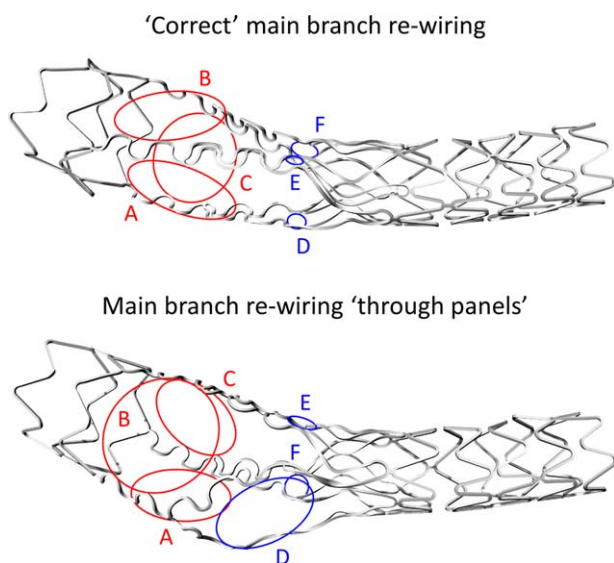


FIGURE 7 Tryton stent geometry at the end of the procedure for the two investigated scenarios. The circumferences fitted within the large sized cells of the proximal zone (red) and the panels of the transition zone of the stent (blue) were used to estimate the Tryton cells' opening [Color figure can be viewed at wileyonlinelibrary.com]

Figure 8A compares the two analyzed cases in terms of stress distribution in the arterial wall at the end of the procedure. In both scenarios, the high stress was confined in the proximal main branch, which was characterized by an overexpansion of the vessel due to kissing balloon inflation. The peak wall stress was localized at the side branch ostium opposite to the carina in both cases and was 0.38 MPa in the

TABLE 1 Cell size of the Tryton stent at the end of the stenting procedure for the two investigated scenarios

Tryton stent cell	Cell size (mm)	
	"Correct" MB rewiring	MB rewiring "though a panel"
A	3.40	3.08
B	3.38	3.62
C	3.05	2.99
D	0.59	3.02
E	0.50	0.90
F	0.86	0.83

Tryton cells under investigation are indicated in Figure 4. Table legend: MB = main branch.

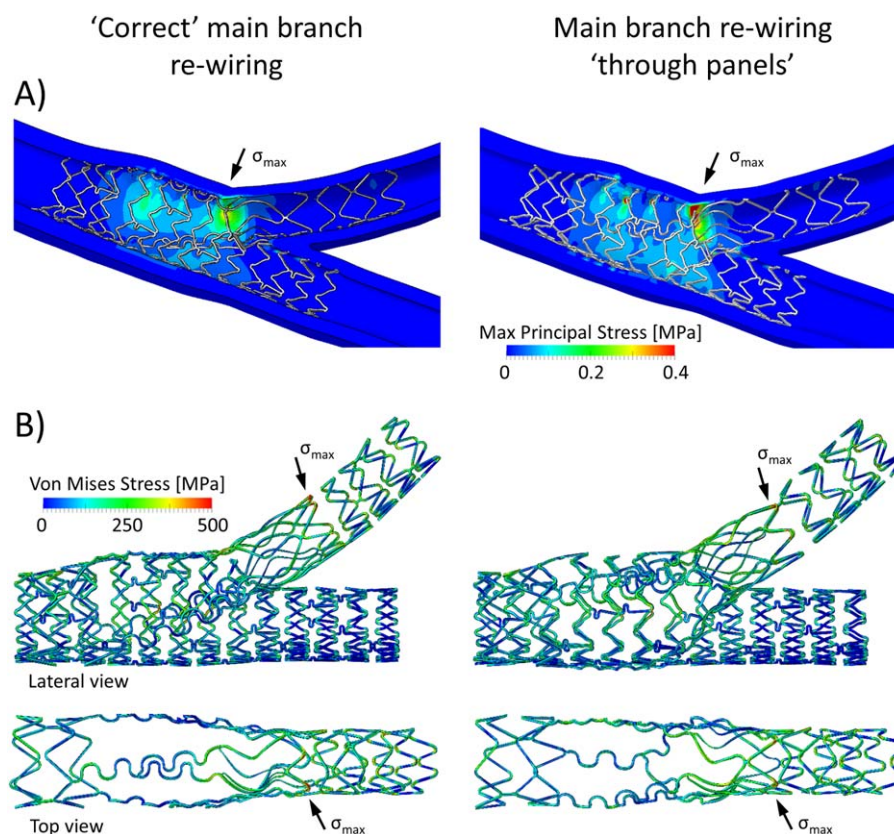


FIGURE 8 Comparison of the two investigated scenarios in terms of biomechanical outcomes at the end of the stenting procedure. A, Contour maps of maximum principal stress in the arterial wall. B, Contour maps of von Mises stress in the two deployed stents (top) and in the Tryton stent (bottom). The locations characterized by peak stress are indicated by black arrows [Color figure can be viewed at wileyonlinelibrary.com]

case with “correct” main branch rewiring and 4.00 MPa in the case with main branch rewiring “through a panel.” Figure 8B shows the distribution of stress in the stents, which was similar in both scenarios. The peak stress occurred in the Tryton stent in both scenarios at the crown of the transition zone that is connected with one link to the distal zone and was 629 MPa with “correct” main branch rewiring and 619 MPa with rewiring “through a panel.”

4 | DISCUSSION

The main findings of the current study are:

1. After Tryton stent implantation, as shown with 3D-OCT, distal main branch re-wiring and subsequently main branch stenting is performed through a Tryton panel (instead of the assumed scenario of rewiring through the large sized cells in-between the panels) in 45% of the evaluated cases.
2. We evaluated the implications of these two clinical scenarios on mechanical stent behavior using virtual stent deployments and we found differences in stent geometries and mechanical stent behavior between the two different clinical scenarios.
3. The main differences with virtual stent deployment were: (a) ostial side branch stenosis of 44.8% (“in-between the panels”) versus

39.0% (“through a panel”); (b) diameter of the largest possible circle that fit the rewired stent cells after main branch implantations of 3.40 mm (“in-between the panels”) versus 3.02 mm (“through a panel”); and (c) peak wall stress which was 0.38 MPa (“in-between the panels”) versus 4.00 MPa (“through a panel”).

In contrast to other dedicated bifurcation stents, such as the Nile-CroCo or Nile-PAX (Minvasys, Gennevilliers, France) [20], the Tryton stent does not need rotational orientation during implantation. However, when analyzing one of the Tryton stent implantations performed in our catheterization lab (Academic Medical Center, Amsterdam, The Netherlands), using 3D-OCT (the case example of Figure 5, Supporting Information video 2), we noticed that after Tryton implantation, one of the panels “blocked” the distal main branch ostium. When carefully analyzing the 3D-OCT reconstruction of the Tryton stent from the main branch pullback after main branch stenting (possible because of the use of Absorb BVS), we noticed that re-wiring and main branch stent placement was performed through one of the panels, instead of the assumed placement through the large cells in-between the panels.

Therefore, we have systematically analyzed the occurrence of this phenomenon by evaluating all 3D-OCT reconstructions available from earlier studies. To our surprise, we found an incidence of 45% of “correct” rewiring and main branch stent placement (through the large sized cells in-between the panels), and 45% of “incorrect” placement

(through the panels). This posed the question whether this was clinically relevant. However, a clinical study to investigate this question necessitates the inclusion of hundreds to thousands of patients to have enough power to evaluate clinical outcomes (such as side branch restenosis) and such a study is not feasible.

As an alternative, we used computer simulations to investigate the influence of the “through a panel” rewiring on the geometry and mechanical behavior and of the Tryton stent. This methodology, known as “virtual bench testing,” has been widely accepted as a valuable alternative to in vitro bench testing [21,22]. The advantages of virtual over traditional bench testing is that it allows the assessment of quantities that are impossible to measure in an experimental bench test environment, such as the stent stress state.

By using virtual bench testing in the current study, we found that the geometrical differences between the two scenarios were only minimal: ostial side branch stenoses were 44.8% (in-between two panels) versus 39.0% (through a panel) and minimum stent areas of the distal main branch ostium were 6.38 mm² (in-between two panels) versus 6.39 mm² (through a panel). Importantly, in both scenarios there was an adequate cell opening for main branch stenting as the diameters of the largest possible circles that fit the re-wired stent cells after main branch implantations were 3.40 mm (in-between two panels) and 3.02 mm (through a panel), which is sufficient for the 2.76 mm distal main branch diameter. Therefore, it is unlikely that the “napkin ring” effect will occur in both scenarios [3,4].

Areas of high stent stresses are associated with stent strut fractures [23]. However, the fenestration of the panel in the rewiring “through a panel” scenario did not lead to excessive peak stresses of the stent. In both scenarios, the peak stent stresses remained lower than the ultimate tensile strength of the cobalt-chromium alloy (~1 GPa [24]). Thus, the Tryton stent did not break during the implantation steps. Because the panels showed large deformations in the scenario in which rewiring was performed through the panel, we would have expected critical stress values in the transition zone. However, peak stress values were comparable in that region in both scenarios. In both scenarios the highest stresses were located at the crown of the transition zone that is connected with one link to the distal zone (in the side branch ostium opposite to the carina) (Figure 8B). It is therefore unlikely that strut fractures will occur more often in the rewiring “through panel” scenario after implantation, although formally, this will need a fatigue testing study.

Our article has several limitations. The clinical OCT data used in this study was obtained in only 11 patients in one center. Our findings may not be generalizable to all procedures performed with the Tryton stent and rewiring through the panels may occur less frequently. We used an idealized bifurcation model without stenosis. It is conceivable that stenosis and plaque content (lipid-rich plaques versus calcified plaques, for instance) would yield different results. We were not able to investigate the influence of the two scenarios on clinical outcomes directly. For such an analysis, hundreds to thousands of patients are needed. Furthermore, this analysis is complicated by the inability to distinguish the Tryton stent from a metallic main branch stent. We were able to investigate Tryton rewiring because of the use of BVS as main

branch stent. However, with the more recent reports of increased risk of stent thrombosis with BVS [25,26], its use is no longer recommended, which will hamper future in vivo studies on Tryton rewiring.

5 | CONCLUSIONS

The Tryton stent is implanted without the need for rotational orientation. However, we found in 11 patients that distal main branch rewiring and subsequent main branch stent implantation may occur through one of the Tryton panels, instead of the assumed implantation through the large sized cell of its proximal portion, in-between the panels. This difference in rewiring resulted in subtle differences in stent geometries and mechanical stent behavior, as evaluated using computational models of stent deployment. Additional studies are needed to investigate whether these differences will influence clinical outcomes on the long-term.

ORCID

Maik J. Grundeken  <http://orcid.org/0000-0003-2068-3833>

Claudio Chiastra  <http://orcid.org/0000-0003-2070-6142>

REFERENCES

- [1] Grundeken MJ, Stella PR, Wykrzykowska JJ. The Tryton Side Branch Stent™ for the treatment of coronary bifurcation lesions. *Expert Rev Med Devices* 2013;10:707–716. <https://doi.org/10.1586/17434440.2013.848165>.
- [2] Grundeken MJ, G  n  reux P, Wykrzykowska JJ, Leon MB, Serruys PW. The Tryton side branch stent. *EuroIntervention* 2015;11(Suppl 5):V145–V146. <https://doi.org/10.4244/EIJV11SVA33>.
- [3] Hikichi Y, Inoue T, Node K. Benefits and limitations of cypher stent-based bifurcation approaches: In vitro evaluation using micro-focus CT scan. *J Interv Cardiol* 2009;22:128–134. <https://doi.org/10.1111/j.1540-8183.2009.00442.x>.
- [4] Murasato Y, Hikichi Y, Horiuchi M. Examination of stent deformation and gap formation after complex stenting of left main coronary artery bifurcations using microfocus computed tomography. *J Interv Cardiol* 2009;22:135–144. <https://doi.org/10.1111/j.1540-8183.2009.00436.x>.
- [5] Foin N, Secco GG, Ghilencea L, Krams R, Di Mario C. Final proximal post-dilatation is necessary after kissing balloon in bifurcation stenting. *EuroIntervention* 2011;7:597–604. <https://doi.org/10.4244/EIJV7ISA96>.
- [6] Grundeken MJ, Garcia-Garcia HM, Kraak RP, Woudstra P, de Bruin DM, van Leeuwen TG, Koch KT, Tijssen JG, de Winter RJ, Wykrzykowska JJ. Side branch healing patterns of the Tryton dedicated bifurcation stent: A 1-year optical coherence tomography follow-up study. *Int J Cardiovasc Imaging* 2014;30:1445–1456. <https://doi.org/10.1007/s10554-014-0504-y>.
- [7] Grundeken MJ, Hassell MECJ, Kraak RP, de Bruin DM, Koch KT, Henriques JPS, van Leeuwen TG, Tijssen JGP, Piek JJ, de Winter RJ, Wykrzykowska JJ. Treatment of coronary bifurcation lesions with the Absorb bioresorbable vascular scaffold in combination with the Tryton dedicated coronary bifurcation stent: Evaluation using two- and three-dimensional optical coherence tomography. *EuroIntervention* 2015;11:877–884. https://doi.org/10.4244/EIJY14M08_15.
- [8] Grundeken MJ, Kraak RP, de Bruin DM, Wykrzykowska JJ. Three-dimensional optical coherence tomography evaluation of a left main bifurcation lesion treated with ABSORB® bioresorbable vascular

- scaffold including fenestration and dilatation of the side branch. *Int J Cardiol* 2013;168:e107–e108. <https://doi.org/10.1016/j.ijcard.2013.07.255>.
- [9] Medrano-Gracia P, Ormiston J, Webster M, Beier S, Young A, Ellis C, Wang C, Smedby Ö, Cowan B. A computational atlas of normal coronary artery anatomy. *EuroIntervention* 2016;12:845–854. <https://doi.org/10.4244/EIJV12I7A139>.
 - [10] Finet G, Gilard M, Perrenot B, Rioufol G, Motreff P, Gavit L, Prost R. Fractal geometry of arterial coronary bifurcations: A quantitative coronary angiography and intravascular ultrasound analysis. *EuroIntervention* 2008;3:490–498.
 - [11] Holzapfel G, Sommer G, Gasser CT, Regitnig P. Determination of layer-specific mechanical properties of human coronary arteries with nonatherosclerotic intimal thickening and related constitutive modeling. *Am J Physiol Heart Circ Physiol* 2005;289:H2048–H2058. <https://doi.org/10.1152/ajpheart.00934.2004>.
 - [12] Morlacchi S, Chiastra C, Gastaldi D, Giancarlo P, Dubini G, Migliavacca F. Sequential structural and fluid Dynamic numerical simulations of a stented bifurcated coronary artery. *J Biomech Eng* 2011;133:121010. <https://doi.org/10.1115/1.4005476>.
 - [13] Morlacchi S, Chiastra C, Cutri E, Zunino P, Burzotta F, Formaggia L, Dubini G, Migliavacca F. Stent deformation, physical stress, and drug elution obtained with provisional stenting, conventional culotte and Tryton-based culotte to treat bifurcations: A virtual simulation study. *EuroIntervention* 2014;9:1441–1453. <https://doi.org/10.4244/EIJV9I12A242>.
 - [14] Chiastra C, Grundeken MJ, Wu W, Serruys PW, de Winter RJ, Dubini G, Wykrzykowska JJ, Migliavacca F. First report on free expansion simulations of a dedicated bifurcation stent mounted on a stepped balloon. *EuroIntervention* 2015;10:e1–e3. <https://doi.org/10.4244/EIJV10I11A226>.
 - [15] Iannaccone F, Chiastra C, Karanasos A, Migliavacca F, Gijsen FJH, Segers P, Mortier P, Verheghe B, Dubini G, D, Beule M, Regar E, Wentzel JJ. Impact of plaque type and side branch geometry on side branch compromise after provisional stent implantation. A simulation study. *EuroIntervention* 2016;13:e236–e245. <https://doi.org/10.4244/EIJ-D-16-00498>.
 - [16] Ormiston JA, Webster MWI, Webber B, Stewart JT, Ruygrok PN, Hatrick RL. The “crush” technique for coronary artery bifurcation stenting: insights from micro-computed tomographic imaging of bench deployments. *JACC Cardiovasc Interv* 2008;1:351–357. <https://doi.org/10.1016/j.jcin.2008.06.003>.
 - [17] Ng J, Foin N, Ang HY, Fam JM, Sen S, Nijjer S, Petraco R, Di Mario C, Davies J, Wong P. Over-expansion capacity and stent design model: An update with contemporary DES platforms. *Int J Cardiol* 2016;221:171–179. <https://doi.org/10.1016/j.ijcard.2016.06.097>.
 - [18] Morlacchi S, Colleoni SG, Cárdenes R, Chiastra C, Diez JL, Larrabide I, Migliavacca F. Patient-specific simulations of stenting procedures in coronary bifurcations: Two clinical cases. *Med Eng Phys* 2013;35:1272–1281. <https://doi.org/10.1016/j.medengphys.2013.01.007>.
 - [19] Grundeken MJ, Agostoni P, Lesiak M, Koch KT, Voskuil M, de Winter RJ, Wykrzykowska JJ, Stella PR. Placement of Tryton side branch stent only: A new treatment strategy for Medina 0,0,1 coronary bifurcation lesions. *Catheter Cardiovasc Interv* 2013;82:E395–E402. <https://doi.org/10.1002/ccd.24811>.
 - [20] Berland J. The Nile CroCo and Nile PAX stents. *EuroIntervention* 2015;11:V149–V150. <https://doi.org/10.4244/EIJV11SVA35>.
 - [21] Antoniadis AP, Mortier P, Kassab G, Dubini G, Foin N, Murasato Y, Giannopoulos AA, Tu S, Iwasaki K, Hikichi Y, Migliavacca F, Chiastra C, Wentzel JJ, Gijsen F, Reiber JHC, Barlis P, Serruys PW, Bhatt DL, Stankovic G, Edelman ER, Giannoglou GD, Louvard Y, Chatzizisis YS. Biomechanical modeling to improve coronary artery bifurcation stenting: Expert review document on techniques and clinical implementation. *JACC Cardiovasc Interv* 2015;8:1281–1296. <https://doi.org/10.1016/j.jcin.2015.06.015>.
 - [22] Migliavacca F, Chiastra C, Chatzizisis YS, Dubini G. Virtual bench testing to study coronary bifurcation stenting. *EuroIntervention* 2015;11:V31. <https://doi.org/10.4244/EIJV11SVA7>.
 - [23] Everett KD, Conway C, Desany GJ, Baker BL, Choi G, Taylor CA, Edelman ER. Structural mechanics predictions relating to clinical coronary stent fracture in a 5 year period in FDA MAUDE database. *Ann Biomed Eng* 2016;44:391–403. <https://doi.org/10.1007/s10439-015-1476-3>.
 - [24] Poncin P, Millet C, Chevy J, Proft JL. Comparing and optimizing Co-Cr tubing for stent applications. In Helmus M, Medlin D, editors. *Med. Device Mater. II—Proc. Mater. Process. Med. Devices Conf.*; 2004, pp 27983. <https://doi.org/0871708248>.
 - [25] Ali ZA, Serruys PW, Kimura T, Gao R, Ellis SG, Kereiakes DJ, Onuma Y, Simonton C, Zhang Z, Stone GW. 2-year outcomes with the Absorb bioresorbable scaffold for treatment of coronary artery disease: A systematic review and meta-analysis of seven randomised trials with an individual patient data substudy. *Lancet (London, England)* 2017;390:760–772. [https://doi.org/10.1016/S0140-6736\(17\)31470-8](https://doi.org/10.1016/S0140-6736(17)31470-8).
 - [26] Wykrzykowska JJ, Kraak RP, Hofma SH, van der Schaaf RJ, Arkenbout EK, IJsselmuiden AJ, Elias J, van Dongen IM, Tijssen RYG, Koch KT, Baan J, Vis MM, de Winter RJ, Piek JJ, Tijssen JGP, Henriques JPS, AIDA Investigators. Bioresorbable scaffolds versus metallic stents in routine PCI. *N Engl J Med* 2017;376:2319–2328. <https://doi.org/10.1056/NEJMoa1614954>.

SUPPORTING INFORMATION

Additional Supporting Information may be found online in the supporting information tab for this article.

How to cite this article: Grundeken MJ, Chiastra C, Wu W, et al. Differences in rotational positioning and subsequent distal main branch rewiring of the Tryton stent: An optical coherence tomography and computational study. *Catheter Cardiovasc Interv*. 2018;92:897–906. <https://doi.org/10.1002/ccd.27567>